A MICROANALYTICAL STUDY OF SECONDARY PRECIPITATION IN RSR 143 USING ATOM PROBE FIELD ION MICROSCOPY AND ANALYTICAL TRANSMISSION ELECTRON MICROSCOPY

M.E. Twigg*, A.J. Melmed*, R. Klein*, M.J. Kaufman**, and H.L. Fraser**

*Surface Science Division, National Bureau of Standards, Washington, D.C. 20234

**Department of Metallurgy and Mining, University of Illinois, Urbana, IL 61801

Summary

For a given heat treatment, the Ni-base superalloy RSR 143 consists of three phases: the γ matrix, γ' cuboids, and DO_{22} platelets. Atom probe field ion microscopy and analytical transmission electron microscopy are used in determining the compositions of these three phases. The most significant result derived from this analysis is the conclusion that both Al and Ta play a direct role in stabilizing the DO_{22} phase in this alloy.

Introduction

At temperatures below 800°C, RSR 143 (76Ni-13Al-9Mo-2Ta, at. %) exhibits a 20 % improvement in stress capability over directionally solidified Mar-M200. Pearson et al. have ascribed this improvement to fine scale secondary precipitates and have recommended the stabilization of these precipitates through compositional modification of the alloy (1). Such an objective in alloy design would be more easily accomplished if the composition of the precipitates and the surrounding γ matrix were known and if the kinetics for formation and dissolution of such precipitates were understood. The question of kinetics has been addressed in an extensive transmission electron microscopy (TEM) study by Martin et al.(2,3). The small size of these secondary precipitates precludes the determination of such compositions through current analytical TEM techniques. These compositions can, however, be determined using atom probe field ion microscopy (APFIM), the principal technique employed in this study.

Experimental

The heat treatment for RSR 143 chosen for the purpose of this analysis was taken from one of the cases examined by Martin (3). The sample used here, a slice from a single crystal of RSR 143, was solution treated in vacuum at 1300°C for 1 hour and then quenched to ambient temperature. Subsequently, the sample was held at a temperature of 800°C for 100 hours. As confirmed by TEM observations, this heat treatment resulted in a large volume fraction of secondary precipitates of the DO_{22} structure; no precipitates of structures D1a or Pt_2Mo were observed. The DO_{22} phase precipitated as platelets on the {100} faces of the cuboidal γ' particles and in the γ matrix. Evidence of these precipitates can be seen in Figs. 1a and 1b.

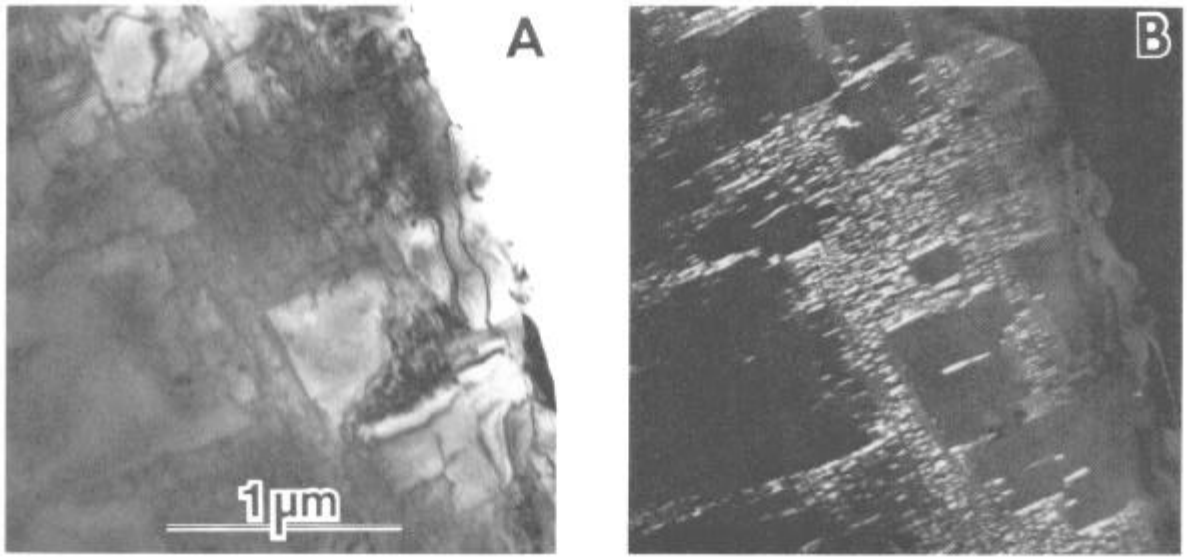

Figure 1. Transmission electron micrographs of RSR 143. a) Bright field micrograph. The 0.5 μ to 0.1 μ cuboids are γ' precipitates set in the γ matrix. b) Dark field micrograph. The bright, finely dispersed particles set in the γ matrix are DO_{22} platelets.

The three phases occurring in the RSR 143 crystal subjected to the above heat treatment were found to be easily distinguishable from one another when imaged in the field ion microscope (FIM). From Figs. 2a, 2b, and 2c, we see that the DO_{22} phase appeared as a bright and very ordered region whereas the γ phase appeared as bright but less ordered in FIM specimens imaged in Ne and cooled by liquid N_2. In Fig. 2d we see that the γ' cuboids imaged less brightly under the same imaging conditions. The γ' phase appeared more ordered than the γ phase, though less ordered than the DO_{22} phase.

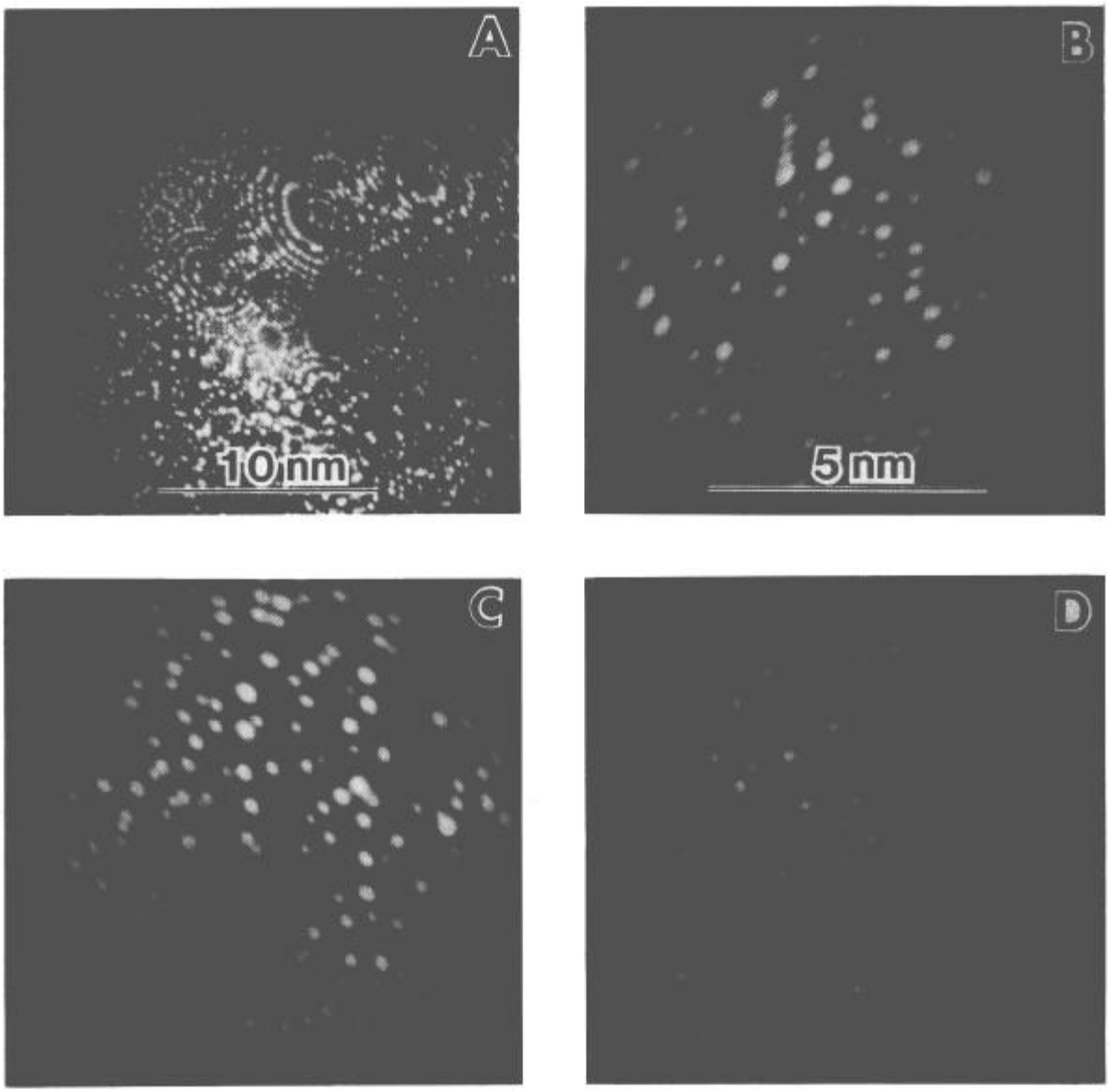

Figure 2. Field ion micrographs of RSR 143 imaged in Ne at a specimen temperature of 80°K. a) Highly ordered DO_{22} platelet against background of less ordered γ matrix. b) DO_{22} phase. c) γ phase. d) γ' phase. The micrographs in Figs. 2b, 2c, and 2d are of the same magnification.

Microelemental analysis using the APFIM revealed the composition of the DO_{22} phase as 76Ni-4Al-17Mo-3Ta (at.%). The composition of the surrounding γ matrix was found to be 80Ni-13Al-7Mo. Transmission electron microscopy revealed the size of the γ' cuboids to be on the order of .5μ; large enough for composition determination by analytical TEM techniques. Using energy dispersive X-ray spectroscopy (EDXS), we found the composition of the γ' to be 69Ni-22Al-4Mo-5Ta (at.%). This composition compares favorably with that obtained using APFIM: 68Ni-26Al-3Mo-3Ta. In Table I, we list the composition for each of the three phases.

Table I. Analysis of RSR 143

	Ni	Al	Mo	Ta
RSR 143	76	13	9	2
DO_{22}, APFIM	76	4	17	3
γ, APFIM	80	13	7	-
γ', APFIM	68	26	3	3
λ', TEM/EDXS	69	22	4	5

Discussion

It is apparent from the TEM study conducted by Martin (3) that the DO_{22} phase is very stable in RSR 143 held at 800°C. According to van Tendeloo et al. (4), however, in an alloy of composition Ni_3Mo, the DO_{22} phase dissolves in 5 minutes when held at 800° C. One might suppose then, that additions of Al and Ta play some role in enhancing the stability of the DO_{22} phase. Because the ordered DO_{22} phase is based on the same fcc lattice as the γ matrix and the γ' precipitates, Martin discussed this role in terms of the statistical theory of long-range order (LRO) developed by de Fontaine (5).

In many theoretical treatments, it is assumed that LRO occurs when an atom of a given species is more strongly attracted to atoms of a different species than to atoms of its own species. One might also guess that the structure of the resulting LRO might be influenced by the relative strength of second nearest neighbor bonds as compared to first nearest neighbor bonds. Indeed, the average pairwise interaction energy existing between i^{th} nearest neighbors is regarded as the fundamental parameter influencing LRO in alloy systems. For a binary alloy system composed of atomic species A and B, the average pairwise interaction energy for i^{th} nearest neighbors is

$$V_i = \frac{1}{2}(V_i^{AA} + V_i^{BB} - 2V_i^{AB}). \qquad (1)$$

Here V_i^{AA} and V_i^{BB} are the pairwise interaction energies for like i^{th} nearest neighbors. The term V_i^{AB} is the pairwise interaction energy for unlike i^{th} nearest neighbors. The energies V_i^{AA}, V_i^{BB}, and V_i^{AB} are negative quantities which become increasingly negative as the bond in question strengthens. In order to favor unlike i^{th} nearest neighbors, V_i must then be positive.

The significance of the average pairwise interaction energies for first and second nearest neighbors (V_1 and V_2) in ordering reactions can be seen in terms of their effect on atomic scale composition modulations. The DO_{22} phase can be described by two sets of standing waves corresponding to composition modulations on an atomic scale: the $\langle 1\frac{1}{2}0\rangle$ waves and the $\langle 100\rangle$ waves. The presence of these modulations is obvious from the transmission electron diffraction pattern of the DO_{22} phase in Fig. 3a. According to de Fontaine (5), the $\langle 1\frac{1}{2}0\rangle$ modulation is favored for $0 \leq V_2/V_1 \leq 0.5$, whereas the $\langle 100\rangle$ modulation is favored for $V_2/V_1 \leq 0$. For both $\langle 1\frac{1}{2}0\rangle$ and $\langle 100\rangle$ modulations, $V_1 > 0$. According to Moss and Clapp (6), x-ray diffraction measurements of Spruiell and Stansbury (7) indicate that $V_2/V_1 = 0.3$ for Ni-Mo alloys. For the same alloy system, Das et al. (8), using transmission electron diffraction, found that $V_2/V_1 = 0.4$. One would then presume that the instability of the DO_{22} phase in the Ni_3Mo alloy was due to a value of V_2/V_1 too large to allow a stable $\langle 100\rangle$ wave to develop.

The V_2/V_1 ratio in a Ni-Mo alloy could be lowered by adding a small concentration of a third element known to lower V_2/V_1 in another Ni-base alloy system. It is well known that alloy phases of nominal composition Ni_3Al (such as the γ' cuboids in RSR 143) are of the $L1_2$ structure. As the presence of $\langle 100\rangle$ reflections in the diffraction pattern for the γ' cuboids in Fig. 3b indicates, $\langle 100\rangle$ concentration modulations order the $L1_2$ superlattice. In order for the $\langle 100\rangle$ modulation in this phase to exist, however, V_2/V_1 must be less than zero. Therefore, substituting Al for some of the Mo in the DO_{22} phase would lower V_2/V_1 and in so doing enhance the stability of the $\langle 100\rangle$ modulation. Because Ni_3Ta has a high temperature DO_{22} phase, the addition of Ta would also be expected to lower V_2/V_1 and stabilize the $\langle 100\rangle$ modulation (5). Clearly, these scenarios for stabilizing the DO_{22} phase are in accord with the observed composition of 76Ni-4Al-17Mo-3Ta.

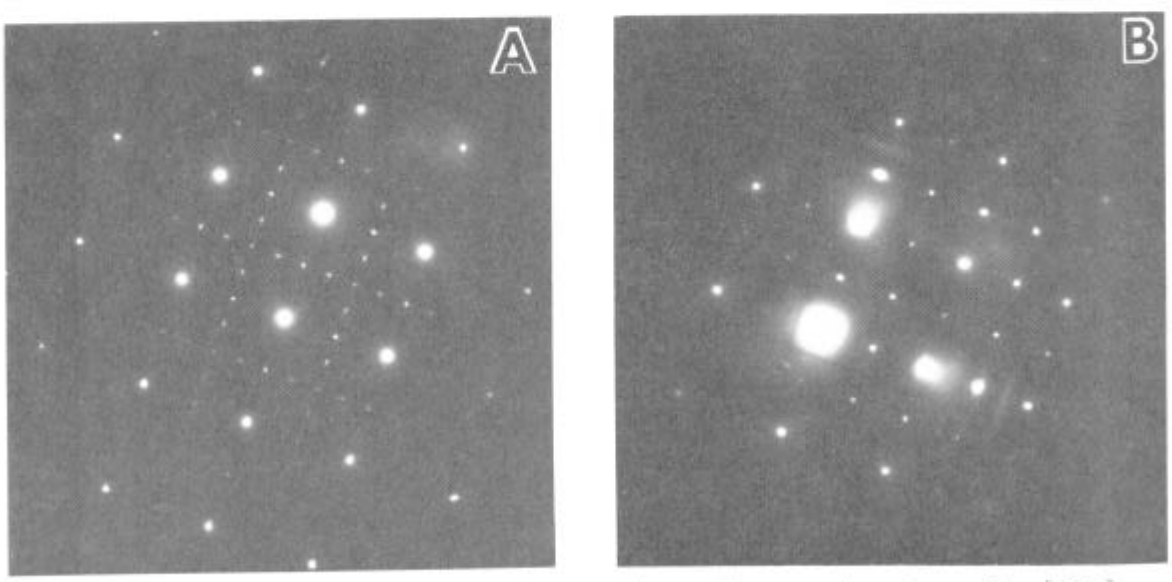

Figure 3. Transmission electron diffraction patterns viewed on the [100] zone axis. a) Selected area diffraction pattern for a region of the γ matrix containing DO_{22} platelets. The $\langle 1\frac{1}{2}0\rangle$ and $\langle 100\rangle$ superlattice reflections correspond to composition modulations in the $\langle 1\frac{1}{2}0\rangle$ and $\langle 100\rangle$ directions. b) Selected area diffraction pattern for a $\gamma'(L1_2)$ cuboidal precipitate. The $\langle 100\rangle$ superlattice reflections correspond to composition modulations in $\langle 100\rangle$ directions.

Acknowledgements

We would like to thank Dr. Nancy Tighe and Dr. Robert Mehrabian for use of the transmission electron microscope operated by the Center for Materials Science at the National Bureau of Standards.

References

1. D. D. Pearson, B. H. Kear, and F. D. Lemkey, "Factors Controlling the Creep Behavior of a Nickel-Base Superalloy," pp. 213-233 in Creep and Fracture of Engineering Materials and Structures, B. Wilshire and D. R. J. Owen, eds.; Pineridge Press, Swansea, U.K., 1981.

2. P. L. Martin, H. A. Lipsitt, and J. C. Williams, "The Structure of As-Extruded RSR Ni-Al-Mo and Ni-Al-Mo-X alloys," pp. 123-128 in Rapid Solidification Processing Principles and Technologies II, R. Mehrabian, B. H. Kear, and M. Cohen, eds.; Claitors, Baton Rouge, La., 1980.

3. P. L. Martin, Ordering Reactions in Ni-Mo Based Alloys, Ph.D. Thesis, Carnegie-Melbon University, Pittsburgh, Pa., 1982.

4. G. van Tendeloo, R. De Ridder, and S. Amelinckx, "The DO_{22} Intermediate Phase in the Ni-Mo System", Physica Status Solidi (a), 27(2) (1975) pp. 457-468.

5. D. de Fontaine, "k-Space Symmetry Rules for Order-Disorder Reactions," Acta Metallurgica, 23 (1) (1975) pp. 553-571.

6. S. C. Moss and P. C. Clapp, "Correlation Functions of Disordered Binary Alloys III," Physical Review, 171 (3) (1968), pp. 764-777.

7. J. E. Spruiell and E. E. Stansbury, "X-Ray Studies of Short-Range Order in Nickel Alloys Containing 10.7 and 20.0 at.% Molybdenum," Journal of Physics and Chemistry of Solids, 26 (1) (1956), pp. 811-822.

8. S. K. Das, P. R. Okamoto, P. M. J. Fisher, and G. Thomas, "Short Range Order in Ni-Mo, Au-Cr, Au-V, and Au-Mn Alloys," Acta Metallurgica, 21 (7) (1973), pp. 913-928.